

# Fundamental limits on the rate of bacterial cell division

<sup>3</sup> **Nathan M. Belliveau<sup>†, 1</sup>, Griffin Chure<sup>†, 2, 3</sup>, Christina L. Hueschen<sup>4</sup>, Hernan G.  
<sup>4</sup> Garcia<sup>5</sup>, Jané Kondev<sup>6</sup>, Daniel S. Fisher<sup>7</sup>, Julie Theriot<sup>1, 8</sup>, Rob Phillips<sup>2, 9, \*</sup>**

\*For correspondence:

<sup>†</sup>These authors contributed equally to this work

<sup>5</sup> <sup>1</sup>Department of Biology, University of Washington, Seattle, WA, USA; <sup>2</sup>Division of  
<sup>6</sup> Biology and Biological Engineering, California Institute of Technology, Pasadena, CA,  
<sup>7</sup> USA; <sup>3</sup>Department of Applied Physics, California Institute of Technology, Pasadena, CA,  
<sup>8</sup> USA; <sup>4</sup>Department of Chemical Engineering, Stanford University, Stanford, CA, USA;  
<sup>9</sup> <sup>5</sup>Department of Molecular Cell Biology and Department of Physics, University of  
<sup>10</sup> California Berkeley, Berkeley, CA, USA; <sup>6</sup>Department of Physics, Brandeis University,  
<sup>11</sup> Waltham, MA, USA; <sup>7</sup>Department of Applied Physics, Stanford University, Stanford, CA,  
<sup>12</sup> USA; <sup>8</sup>Allen Institute for Cell Science, Seattle, WA, USA; <sup>9</sup>Department of Physics,  
<sup>13</sup> California Institute of Technology, Pasadena, CA, USA; \*Contributed equally

<sup>14</sup> 

---

<sup>15</sup> **Abstract** This will be written next (promise).

<sup>16</sup> 

---

## <sup>17</sup> Translation and ribosomal synthesis

<sup>18</sup> Lastly, we turn our attention to the process of synthesizing new proteins, translation. This process  
<sup>19</sup> stands as a good candidate for potentially limiting growth since the synthesis of new proteins relies  
<sup>20</sup> on the generation of ribosomes, themselves proteinaceous molecules. As we will see in the coming  
<sup>21</sup> sections of this work, this poses a "chicken-or-the-egg" problem where the synthesis of ribosomes  
<sup>22</sup> requires ribosomes in the first place.

<sup>23</sup> We will begin our exploration of protein translation in the same spirit as we have in previous sec-  
<sup>24</sup> tions – we will draw order-of-magnitude estimates based on our intuition and available literature,  
<sup>25</sup> and then compare these estimates to the observed data. In doing so, we will estimate both the  
<sup>26</sup> absolute number of ribosomes necessary for replication of the proteome as well as the synthesis  
<sup>27</sup> of amino-acyl tRNAs. From there we consider the limitations on ribosomal synthesis in light of our  
<sup>28</sup> estimates on both the synthesis of ribosomal proteins and our earlier results on rRNA synthesis.

## <sup>29</sup> tRNA synthetases

<sup>30</sup> We begin by first estimating the number of tRNA synthetases in *E. coli* needed to convert free amino-  
<sup>31</sup> acids to polypeptide chains. At a modest growth rate of  $\approx 5000$  s, *E. coli* has roughly  $3 \times 10^6$  proteins  
<sup>32</sup> per cell (BNID: 115702; *Milo et al. (2010)*). Assuming that the typical protein is on the order of  $\approx$   
<sup>33</sup> 300 amino acids in length (BNID: 100017; *Milo et al. (2010)*), we can estimate that a total of  $\approx 10^9$   
<sup>34</sup> amino acids are stitched together by peptide bonds.

<sup>35</sup> How many tRNAs are needed to facilitate this remarkable number of amino acid delivery events  
<sup>36</sup> to the translating ribosomes? It is important to note that tRNAs are recycled after they've passed  
<sup>37</sup> through the ribosome and can be recharged with a new amino acid, ready for another round of  
<sup>38</sup> peptide bond formation. While some *in vitro* data exists on the turnover of tRNA in *E. coli* for  
<sup>39</sup> different amino acids, we can make a reasonable estimate by comparing the number of amino  
<sup>40</sup> acids to be polymerized to cell division time. Using our stopwatch of 5000 s and  $10^9$  amino acids,  
<sup>41</sup> we arrive at a requirement of  $\approx 2 \times 10^5$  tRNA molecules. This estimate is in line with experimental

42 measurements of  $\approx 3 \times 10^5$  per cell (BNID: 108611, *Milo et al. (2010)*), suggesting we are on the  
43 right track.

44 There are many processes which go into synthesizing a tRNA and ligating it with the appropriate  
45 amino acids. As we covered in the previous section, there appear to be more than enough RNA  
46 polymerases per cell to synthesize the needed pool of tRNAs. Without considering the many ways  
47 in which amino acids can be scavenged or synthesized *de novo*, we can explore ligation the as a  
48 potential rate limiting step. The enzymes which link the correct amino acid to the tRNA, known as  
49 tRNA synthetases or tRNA ligases, are incredible in their proofreading of substrates with the incor-  
50 rect amino acid being ligated once out of every  $10^4$  to  $10^5$  times (BNID: 103469, *Milo et al. (2010)*).  
51 This is due in part to the consumption of energy as well as a multi-step pathway to ligation. While  
52 the rate at which tRNA is ligated is highly dependent on the identity of the amino acid, it is reason-  
53 able to state that the typical tRNA synthetase has charging rate of  $\approx 20$  AA per tRNA synthetase per  
54 second (BNID: 105279, *Milo et al. (2010)*).

55 Combining these estimates together, as shown schematically in *Figure 1(A)*, yields an estimate  
56 of  $\approx 10^4$  tRNA synthetases per cell with a division time of 5000 s. This point estimate is in very close  
57 agreement with the observed number of synthetases (the sum of all 20 tRNA synthetases in *E. coli*).  
58 This estimation strategy seems to adequately describe the observed growth rate dependence of  
59 the tRNA synthetase copy number (shown as the grey line in *Figure 1(B)*), suggesting that the copy  
60 number scales with the cell volume.

61 In total, the estimated and observed  $\approx 10^4$  tRNA synthetases occupy only a meager fraction of  
62 the total cell proteome, around 0.5% by abundance. It is reasonable to assume that if tRNA charg-  
63 ing was a rate limiting process, cells would be able to increase their growth rate by devoting more  
64 cellular resources to making more tRNA synthases. As the synthesis of tRNAs and the correspond-  
65 ing charging can be highly parallelized, we can argue that tRNA charging is not a rate limiting step  
66 in cell division, at least for the growth conditions explored in this work.

### 67 Protein synthesis

68 With the number of tRNA synthetases accounted for, we now consider the abundance of the pro-  
69 tein synthesis machines themselves, ribosomes. Ribosomes are enormous protein/rRNA com-  
70 plexes that facilitate the peptide bond formation between amino acids in the correct sequence  
71 as defined by the coding mRNA. Before we examine the synthesis of the ribosome proteins and  
72 the limits that may place on the observed bacterial growth rates, let's consider replication of the  
73 cellular proteome.

74 As described in the previous section, an *E. coli* cell consisting of  $\approx 3 \times 10^6$  proteins will have  
75 on the order  $\approx 10^9$  peptide bonds per proteome. While the rate at which ribosomes translates is  
76 well known to have a growth rate dependence *Dai et al. (2018)* and is a topic which we discuss in  
77 detail in the coming sections. However, for the purposes of our order-of-magnitude estimate, we  
78 can make the approximation that translation occurs at a rate of  $\approx 15$  amino acids per second per  
79 ribosome (BNID: 100233, *Milo et al. (2010)*). Under this approximation and assuming a division  
80 time of 5000 s, we can arrive at an estimate of  $\approx 10^4$  ribosomes are needed to replicate the cellular  
81 proteome, shown in *Figure 1(B)*. This point estimate, while glossing over important details such  
82 as chromosome copy number and growth-rate dependent translation rates, proves to be notably  
83 accurate when compared to the experimental observations (*Figure 1(B)*).

### 84 Translation as a growth-rate limiting step

85 Thus far, the general back-of-the-envelope estimates have been reasonably successful in explain-  
86 ing what sets the scale of absolute protein copy number. A recurring theme that has arisen is the  
87 ability of cells to parallelize their biosynthesis tasks. For example, while DNA replication speed-limit  
88 is  $\approx 40$  minutes to replicate a genome, cells can divide faster than this by initiating more than one  
89 round of replication per doubling. However, as we will see, parallelization is not possible when it  
90 comes to the translation of ribosomal proteins (*Figure 2(A)*). Thus, it is plausible that translation

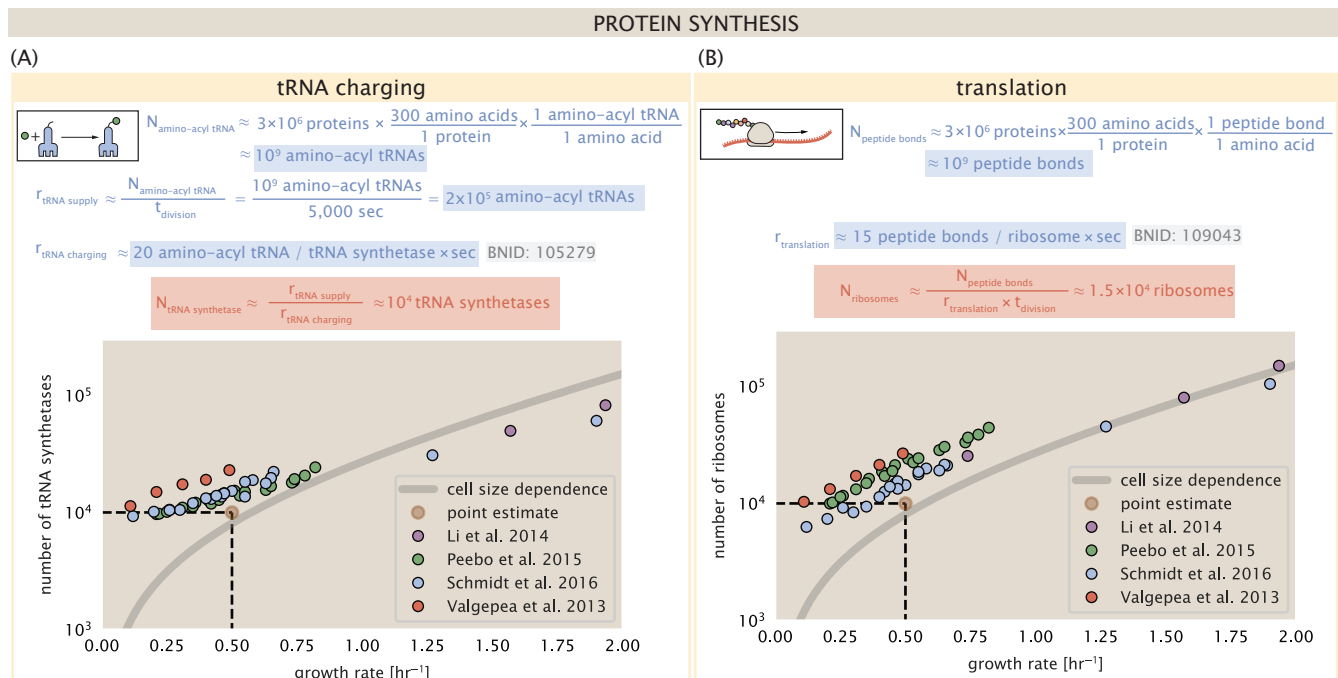


**Figure 1. Estimation of the required tRNA synthetases and ribosomes.** (A) Estimation for the number of tRNA synthetases that will supply the required amino acid demand. The sum of all tRNA synthetases copy numbers are plotted as a function of growth rate ([ArgS], [CysS], [GlnS], [Glx], [IleS], [LeuS], [ValS], [AlaS]<sub>2</sub>, [AsnS]<sub>2</sub>, [AspS]<sub>2</sub>, [TyrS]<sub>2</sub>, [TrpS]<sub>2</sub>, [ThrS]<sub>2</sub>, [SerS]<sub>2</sub>, [ProS]<sub>2</sub>, [PheS]<sub>2</sub>[PheT]<sub>2</sub>, [MetG]<sub>2</sub>, [LysS]<sub>2</sub>, [HisS]<sub>2</sub>, [GlyS]<sub>2</sub>[GlyQ]<sub>2</sub>). (B) Estimation of the number of ribosomes required to synthesize 10<sup>9</sup> peptide bonds with an elongation rate of 15 peptide bonds per second. The average abundance of ribosomes is plotted as a function of growth rate. Our estimated values are shown for a growth rate of 0.5 hr<sup>-1</sup>. Grey lines correspond to the estimated complex abundance calculated at different growth rates. See Supplemental Information XX for a more detail description of this calculation.

91 may be a key factor in determining the cellular growth rate.

92 To gain some intuition into how translation can set the speed of bacterial growth, we again  
 93 consider the total number of peptide bonds that must be synthesized, which we denote as  $N_{AA}$ .  
 94 Noting that cells grow exponentially in time (**Godin et al., 2010**), we can compute the number of  
 95 amino acids to be polymerized as

$$N_{AA}\lambda = r_t R, \quad (1)$$

96 where  $\lambda$  is the cell growth rate in  $s^{-1}$ ,  $r_t$  is the maximum translation rate in  $AA \cdot s^{-1}$ , and  $R$  is the  
 97 average ribosome copy number per cell. Knowing the number of peptide bonds to be formed  
 98 permits us to compute the translation-limited growth rate as

$$\lambda_{\text{translation-limited}} = \frac{r_t R}{N_{AA}}. \quad (2)$$

99 Alternatively, since  $N_{AA}$  is related to the total protein mass through the molecular weight of  
 100 each protein, we can also consider the growth rate in terms of the fraction of the total proteome  
 101 mass that is dedicated to ribosomal protein mass. By making the approximation that an average  
 102 amino acid has a molecular weight of 110 Da (BNID: 104877, **Milo et al. (2010)**), we can approximate  
 103  $R/N_{AA} \approx \Phi_R/L_R$ , where  $\Phi_R$  is the ribosomal mass fraction and  $L_R$  is the total length in amino acids  
 104 that make up a ribosome. The translation-limited growth rate can then be written in the form

$$\lambda_{\text{translation-limited}} \approx \frac{r_t}{L_R} \Phi_R. \quad (3)$$

105 This is plotted as a function of ribosomal fraction  $\Phi_R$  in **Figure 2(B)**, where we take  $L_R \approx 7500$  AA,  
 106 corresponding to the length in amino acids for all ribosomal subunits of the 50S and 30S complex  
 107 (BNID: 101175, (**Milo et al., 2010**)).

108 The growth rate defined by **Equation 3** reflects mass-balance under steady-state growth and  
 109 has long provided a rationalization of the apparent linear increase in *E. coli*'s ribosomal content  
 110 as a function of growth rate (**Maaløe, 1979; Scott et al., 2010**). We note that there is a maximum  
 111 growth rate of  $\lambda \approx 8 \text{ hr}^{-1}$ , or a doubling time just under 6 minutes (**Figure 2(B)**, dashed line). This  
 112 represents an inherent speed limit due to the need for the cell to double its entire ribosomal mass.  
 113 Interestingly, this limit is independent of the absolute number of ribosomes and is simply given by  
 114 the time to translate an entire ribosome,  $L_R/r_t$ . As shown in **Figure 2(A)**, we can reconcile this with  
 115 the observation that in order to double the average number of ribosomes, each ribosome must  
 116 produce a second ribosome and cannot be parallelized.

117 Earlier, we considered rRNA synthesis (see Section **RNA Synthesis**), finding that, when the rRNA  
 118 operons are maximally loaded with RNA polymerase, the cell can produce  $\approx 1$  functional rRNA unit  
 119 per second per operon. In **Figure 2(C)**, we show the maximum number of ribosomes that could  
 120 be made as a function of growth rate given this rRNA production rule-of-thumb. While each *E.*  
 121 *coli* genome has 7 copies of the rRNA operon (BNID: 107866, **Milo et al. (2010)**), parallelization  
 122 of DNA synthesis by firing multiple rounds of replication at a time can drastically increase the effective  
 123 number of rRNA operons. The blue curve in ??, we assume that the effective number of rRNA  
 124 operons increases in proportion to the number of origins of replication (# ori) (solid blue line;  
 125 with the calculation of (# ori) described in the next section). Although we expect this value to  
 126 drastically overestimate rRNA abundance at slower growth rates ( $\lambda < 0.5 \text{ hr}^{-1}$ ), it provides a useful  
 127 reference when considered along with the proteomic measurements that are also plotted. For  
 128 growth rates above about  $1 \text{ hr}^{-1}$ , we find that cells will need to transcribe rRNA near their maximal  
 129 rate. The dashed blue curve in **Figure 2(C)** shows the maximal number of functional rRNA units  
 130 that could be synthesized from a single genome (ignoring the chromosome replication speed limit  
 131 of  $\approx 40$  minutes per genome). The convergence between the maximum rRNA production with  
 132 parallelization and the experimentally measured ribosome copy number (points in **Figure 2(C)**), as  
 133 well as the observation cells are rarely reported to grow faster than  $2 \text{ hr}^{-1}$  (**Bremer and Dennis,**  
 134 **2008**), suggests rRNA synthesis represents the rate limiting step in cell division for this strain of *E.*  
*coli*.

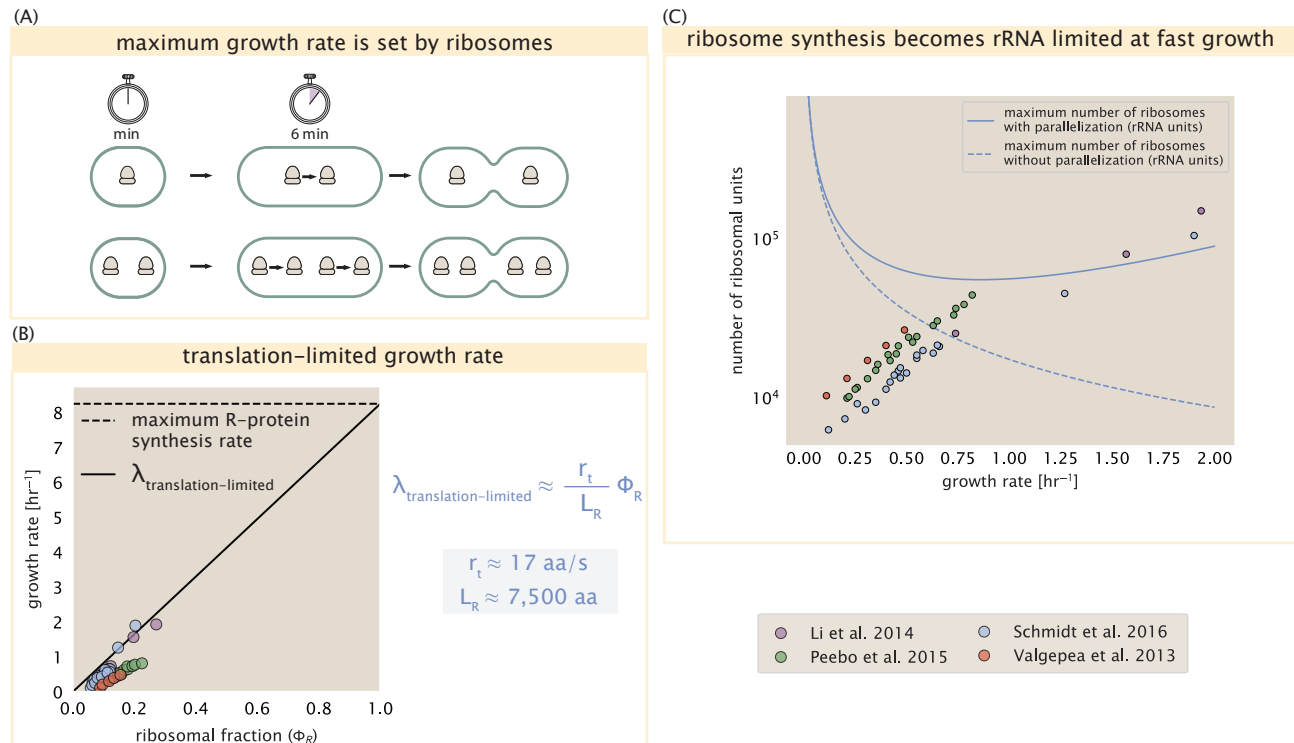


**Figure 2. Translation-limited growth rate.** (A) Here we consider the translation-limited growth as a function of ribosomal fraction. By mass balance, the time required to double the entire proteome ( $N_{AA} / r_t$ ) sets the translation-limited growth rate,  $\lambda_{\text{translation-limited}}$ . Here  $N_{AA}$  is effectively the number of peptide bonds that must be translated,  $r_t$  is the translation elongation rate, and  $R$  is the number of ribosomes. This can also be re-written in terms of the ribosomal mass fraction  $\Phi_R = m_R / m_{\text{protein}}$ , where  $m_R$  is the total ribosomal mass and  $m_{\text{protein}}$  is the mass of all proteins in the cell.  $L_R$  refers to the summed length of the ribosome in amino acids.  $\lambda_{\text{translation-limited}}$  is plotted as a function of  $\Phi_R$  (solid line). (B) The dashed line in part (A) identifies a maximum growth rate that is set by the ribosome. Specifically, this growth rate corresponds to the time required to translate an entire ribosome,  $L_R/r_t$ . This is a result that is independent of the number of ribosomes in the cell as shown schematically here. (C) Maximum number of rRNA units that can be synthesized as a function of growth rate. Solid curve corresponds to the rRNA copy number is calculated by multiplying the number of rRNA operons by the estimated number of (# ori) at each growth rate. The quantity (# ori) was calculated using Equation 4 and the measurements from Si et al. (2017) that are plotted in Figure 3(A). Dashed line show that maximal number of functional rRNA units produced from a single chromosome without parallelization.

**136 Relationship between cell size and growth rate.**

137 With the observation that ribosomes set an inherent upper limit on growth rate, through both rRNA  
 138 synthesis and the additional dependence on ribosomal fraction, it is also plausible that ribosomes  
 139 may play a more dominant role in setting growth rate across other growth conditions. With a rich  
 140 proteomic data set across a wide array of conditions, and in light of a number of recent experi-  
 141 mental observations, we find that cells also appear to tune their ribosomal abundance as a means  
 142 to maximize growth even in poor nutrient conditions. This has important consequences on the  
 143 relationship with cell size and maintenance of steady-state growth. In the coming section and the  
 144 remainder of the text, we consider these further beginning with cell size.

145 The relationship between cell size and growth rate has long been of interest in the study of  
 146 bacterial physiology, particularly following the now six decade-old observation that cell volume  
 147 appears to increase exponentially with growth rate; known as Schaechter's growth law (*Schaechter*  
 148 *et al., 1958; Taheri-Araghi et al., 2015*). Wild-type *E. coli* growing at relatively fast growth rates  
 149 exhibit a remarkably constant cell cycle time  $t_{cyc}$  (referring to the C and D periods of DNA replication  
 150 and cell division, respectively), as shown in *Figure 3(A)* for the data reproduced from *Si et al. (2017)*.  
 151 With a constant cell cycle time, the exponential scaling in size has long been considered a direct  
 152 consequence of cells initiating replication at a constant volume per origin. However, the particular  
 153 mechanism that governs this relationship, and even the question of whether the change in average  
 154 cell size is truly exponential have remained under debate (*Si et al., 2017; Harris and Theriot, 2018*).

155 Since protein accounts for more than half of cellular dry mass (BNID: 104954, *Milo et al. (2010)*;  
 156 *Bremer and Dennis (2008); Basan et al. (2015)*, cell size will vary in proportion to how much protein  
 157 is synthesized over the cell cycle. Through our estimates in the sections on the central dogma, it is  
 158 apparent that the processes of transcription (i.e. synthesis of mRNA) and translation are unlikely  
 159 limiting steps in doubling the cell mass. In both cases, there is an overabundance of the requisite  
 160 protein complexes (DNA and RNA polymerase, respectively) and there are mechanisms by which  
 161 these synthesis processes can be parallelized. Therefore, the total protein mass is determined by  
 162  $r_i \times R$  and the doubling time  $\tau$ . The relationship between cell size and growth rate, however, will  
 163 depend only on how the cell scales its ribosomal fraction  $\Phi_R$ , as highlighted by *Equation 3*.

164 Ribosomal abundance defines exponential scaling between cell size and growth rate  
 165 A naive strategy to increase growth rate given the constraint prescribed by *Equation 3*, would be  
 166 to simply generate more ribosomes. In reality, large swaths of the proteome increases in absolute  
 167 abundance at faster growth (Supplemental Figure X). Substantial empirical evidence has revealed  
 168 a linear scaling between cell size (volume) and the number of chromosomal origins of replication,  
 169  $\langle \# \text{ ori} \rangle$ , which is robust to a remarkable array of perturbations (*Si et al., 2017*). The number of  
 170 origins  $\langle \# \text{ ori} \rangle$  is determined by how often replication must be initiated per cell doubling to maintain  
 171 steady-state growth and can be quantified via

$$\langle \# \text{ ori} \rangle \approx 2^{t_{cyc}/\tau}, \quad (4)$$

172 where  $\tau$  is the doubling time. In *Figure 3(A)*, we show the measurements of *Si et al. (2017)* for wild-  
 173 type *E. coli* cells in nutrient-limit growth regimes. Using this data, we estimated  $\langle \# \text{ ori} \rangle$  for each  
 174 condition in the amalgamated proteomic datasets. With rRNA otherwise becoming rate limited at  
 175 fast growth, this strategy allows for a roughly linear increase in ribosomes copy number with  $\langle \#$   
 176  $\text{ori} \rangle$  as shown in *Figure 3(B)* for the proteomic data.

177 It is notable that in *E. coli*, the majority of ribosomal proteins and rRNA operons are found  
 178 closer to the origin of replication. Since multiple rounds of DNA initiation will effectively skew gene  
 179 dosage in favor of genes near the origin (*Scholz et al., 2019*), it suggests that an increase in  $\langle \# \text{ ori} \rangle$   
 180 is a means to skew the ribosomal fraction of the proteome,  $\Phi_R$ . In *Figure 3(D)* we show that this  
 181 skew in gene dosage is reflected in the composition of the proteome via a running boxcar average  
 182 (500 kbp window) of protein copy number as a function of each gene's transcriptional start site  
 183 (*Figure 3(D)*). While the protein copy numbers of individual proteins can vary substantially across

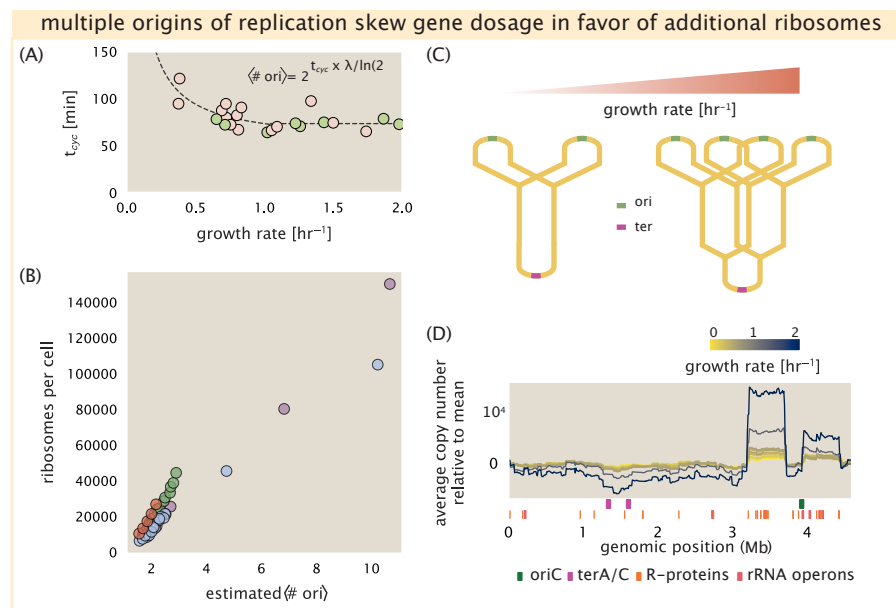


**Figure 3. Multiple replication forks skew gene dosage and ribosomal content.** (A) Experimental data from Si *et al.* (2017). Dashed line shows fit to the data, which were used to estimate  $\langle \# \text{ori} \rangle$ .  $t_{\text{cyc}}$  was assumed to vary in proportion to  $\tau$  for doubling times great than 40 minutes, and then reach a minimum value of [fill in] minutes below this (see Supplemental Appendix X for additional details). Red data points correspond to measurements in strain MG1655, while light green points are for strain NCM3722. (B) Plot of the ribosome copy number estimated from the proteomic data against the estimated  $\langle \# \text{ori} \rangle$  [NB: change to total protein abundance?]. (C) Schematic shows the expected increase in replication forks (or number of ori regions) as *E. coli* cells grow faster. (D) A running boxcar average of protein copy number is calculated for each each growth condition considered by (Schmidt *et al.*, 2016). A 0.5 Mb averaging window was used. Protein copy numbers are reported relative to their condition-specific means in order to center all data sets.

184 the entire chromosome, we nonetheless observe a bias in expression across the chromosome  
 185 under fast growth conditions (dark blue lines) relative to slow growth (yellow lines). The dramatic  
 186 change in protein copy number near the origin is largely due to the increase in ribosomal protein  
 187 expression. This trend is in contrast to slower growth conditions (yellow) where the average copy  
 188 number is much more uniform across the length of the chromosome.

189 This result provides important evidence that although total protein content scales with  $\langle \# \text{ori} \rangle$ , it  
 190 is also the bias in gene dosage for genes closer to the origin that change the proteomic composition  
 191 and allows an increase in the ribosomal fraction  $\Phi_R$  at fast growth. For *E. coli*, we can then view  
 192 the increase in ribosomal fraction  $\Phi_R$  (and therefore,  $\lambda$ ) as requiring a geometric increase in total  
 193 protein abundance that is proportional to  $\langle \# \text{ori} \rangle$ . This leads to an exponential increase in total  
 194 protein mass (and cell size) as long as all ribosomes  $R$  are actively translating protein during cell  
 195 doubling.

196 While our analysis suggests that it is the need to increase the absolute number of ribosomes  
 197 that sets an exponential scaling in cell size, this relationship is likely to falter at slow growth rates  
 198 (below  $\lambda \approx 0.5 \text{ hr}^{-1}$ ). In this regime, ribosome abundance  $R$  no longer reflects the cell's protein syn-  
 199 thesis capacity (Dai *et al.*, 2016), so far taken to be  $r_t \times R$ . Additional regulatory control through the  
 200 small-molecule alarmones such as guanosine pentaphosphate [(p)ppGpp] reduces the fraction of  
 201 actively translating ribosomes at slow growth and yields a translational capacity below  $r_t \times R$ . This  
 202 is why Si *et al.* (2017) found that it was the change in active ribosomal fraction, and not riboso-  
 203 mal fraction alone, that was most consistent with an exponential change in cell size. The specific  
 204 relationship between cell size and growth rate however becomes harder to define because cells  
 205 no longer need multiple rounds of DNA replication to make enough rRNA, and no longer need to  
 206 increase their total protein mass in order to tune protein synthesis. Our collated proteomic data,

however, contain several assumptions that relate total protein abundance to growth rates and this prevents us from making precise predictions about how cell size and absolute protein abundance vary at slow growth (Supplemental X). Nevertheless, we find no evidence that cells decrease their size to the minimal value expected from an exponential function with a constant exponent fit to cell sizes with moderate to fast growth rates (*Basan et al., 2015; JL et al., 2016; Si et al., 2019*), suggesting at least a modified scaling between size and growth rate in these poorer nutrient conditions.

### 214 Growth in poor nutrient conditions.

215 How do cells regulate protein synthesis when amino acids become limiting, meaning that consumption  
 216 exceeds the rate of synthesis? In the slowest growth conditions, we find a minimum ribosomal  
 217 mass fraction of  $\Phi_R \approx 0.06$  and of order  $10^4$  ribosomes per cell. Without the additional regulatory  
 218 control noted above, there would be a point where this imbalance would occur if all ribosomes  
 219 were actively translating (*Figure 4*). Such a scenario would prevent continuous growth, and indeed  
 220 for (p)ppGpp null strains, cells only grow in minimal media if additional amino acid supplements  
 221 are present. In contrast, wild-type *E. coli* maintain a relatively high elongation rate even in stationary  
 222 phase ( $\approx 8$  AA/s, (*Dai et al., 2016, 2018*)).

223 To better understand how regulation of ribosomes influence growth rate at slow growth, we  
 224 consider a coarse-grained model that relates elongation rate to a limiting supply of amino acids,  
 225 which for simplicity we treat as a single, effective rate-limiting species  $[AA]_{eff}$ . Under such a sce-  
 226 nario, the elongation rate  $r_t$  can be described as depending on the maximum elongation rate ( $r_t^{max} \approx$   
 227  $17.1$  AA/s, (*Dai et al., 2016, 2018*)), an effective binding constant  $K_D$  between the pool of amino acids  
 228 and their amino-acyl tRNAs, and the limiting amino acid concentration  $[AA]_{eff}$ ,

$$r_t = r_t^{max} \cdot \frac{1}{1 + K_D/[AA]_{eff}}. \quad (5)$$

229 For cells growing in minimal medium supplemented with glucose, the amino acid concentration is  
 230 of order  $100$  mM (BNID: 110093, (*Milo et al., 2010; Bennett et al., 2009*)). To estimate  $K_D$ , we note  
 231 that for a growth rate of about  $0.6$  hr $^{-1}$  *Dai et al. (2016)* measured an elongation rate of about  $12.5$   
 232 AA·s $^{-1}$ , yielding  $K_D \approx 40$  mM. The maintenance of this amino acid pool  $[AA]_{eff}$  will depend on the  
 233 difference between the synthesis/supply rate of amino acids  $r_{AA}$  and consumption by ribosomes  
 234  $r_t \times R \times f_a$ , where we use  $f_a$  to account for the possible reduction of actively translating ribosomes  
 235 (see Supplemental Appendix XX for further details on this model).

236 In *Figure 4(B)*, we show the relationship between the growth rate and elongation rate as a func-  
 237 tion of the number of actively translating ribosomes. Here, growth rate is now determined by the  
 238 active ribosomal fraction via

$$\lambda_{\text{translation-limited}} \approx \frac{r_t}{L_R} \Phi_R f_a. \quad (6)$$

239 If we consider constant values of amino acid synthesis rate  $r_{AA}$  (dashed lines) to reflect the available  
 240 parameter space for a specific growth condition, the fastest growth rates result from maximization  
 241 of the fraction of actively translating ribosomes. When we consider the experimental measure-  
 242 ments from *Dai et al. (2018)* (yellow circles), reflecting growth in different nutrient conditions, we  
 243 see that although  $R \times f_a$  is reduced in poorer nutrient conditions, it is reduced in a manner such that  
 244  $[AA]_{eff}$  is relatively constant. Given our estimate  $K_D \approx 40$  mM, we would only expect a decrease  
 245 from  $100$  mM to about  $35$  mM in the slowest growth conditions. While experimental data is scarce,  
 246 data from *Bennett et al. (2009)* show that amino acid concentrations only decrease to about  $60$   
 247 mM for cells grown in minimal media supplemented with acetate ( $\lambda \approx 0.3$  hr $^{-1}$  in our proteomic  
 248 data) (*Bennett et al., 2009*), qualitatively consistent with our expectations. One explanation for the  
 249 experimental data is that the active fraction of the ribosome pool is regulated in order to maintain  
 250 a sufficient supply of amino acids for growth. Any further increase in  $R \times f_a$  at constant  $r_{AA}$  would  
 251 otherwise be associated with an additional drop in cellular amino acid concentration.

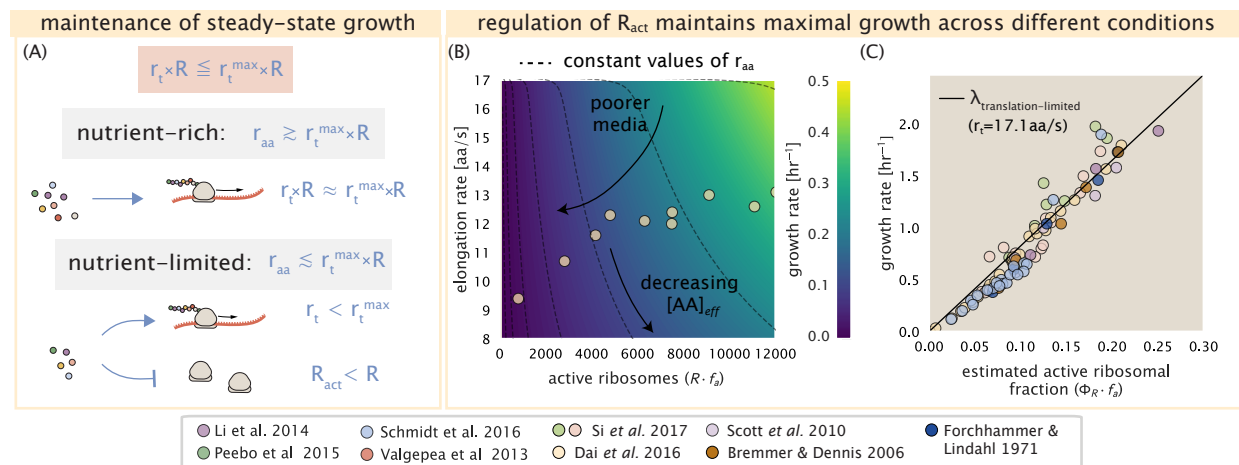


**Figure 4. *E. coli* must regulate ribosomal activity in limiting nutrient conditions.** (A) Schematic showing translation-specific requirements for maintenance of steady-state growth. In a nutrient rich environment, amino acid supply  $r_{aa}$  is sufficiently in excess of the demand by ribosomes translating at their maximal rate. In poorer nutrient conditions, reduced amino acid supply  $r_{aa}$  will decrease the rate of elongation. In a regime where  $r_{aa}$  is less than  $r_t R$ , the number of actively translating ribosomes will need to be reduced in order to maintain steady-state growth. (B) Translation elongation rate is plotted as a function of the number of actively translating ribosomes  $R f_a$ . Dashed lines correspond to a range of amino acid synthesis rates  $r_{aa}$ , from  $10^3$  to  $10^6$ . Growth rates are calculated according to Equation 1, assuming a constant ribosomal fraction of 8 percent. See appendix XX for additional details. (C) Experimental data from (Dai et al., 2016) are used to estimate the fraction of actively translating ribosomes. The solid line represents the translation-limited growth rate for ribosomes elongating at 17.1 AA/s.

252 *E. coli* maximizes its steady-state growth rate by tuning both ribosomal content and trans-  
253 lation activity.

254 Using the active fraction  $f_a$  measurements across a broad range of nutrient-limited growth condi-  
255 tions from the work of Dai et al. (2016), we furthermore estimated the active fraction of ribosomal  
256 protein across the collated proteomic datasets (Figure 4(C)). Importantly, we note that across all  
257 growth conditions considered, cells appear to maintain a growth rate consistent with Equation 3  
258 with an elongation rate of  $r_t \approx 17.1$  AA/s. While somewhat counter intuitive, given that ribosomes  
259 translate at almost half this rate in the poorest of growth conditions, steady-state growth rates can  
260 be achieved over such a broad range of conditions because cells have evolved a means to tune  
261  $r_t \times R \times f_a$ .

262 It has recently been shown that growth in a (p)ppGpp null strain abolishes both the growth-  
263 dependent changes in gene dosage and scaling in cell size. Instead, cells always exhibited a higher  
264 gene dosage near the origin of replication, irrespective of growth rate, and a cell size more  
265 consistent with a fast growth state where (p)ppGpp levels are low (Fernández-Coll et al., 2020) and  
266 ribosomal fraction is high (Zhu and Dai, 2019). This raises the possibility that the action of (p)ppGpp  
267 is also mediating growth control and size scaling over the entire range of growth conditions. Specif-  
268 ically, as nutrient conditions worsen, (p)ppGpp helps decrease multiple rounds of DNA replication  
269 per cell doubling which effectively decreases both  $R$  and the total cell size and in sufficiently poor  
270 growth conditions mitigates translation activity according to nutrient availability.

## References

- 272 Basan, M., Zhu, M., Dai, X., Warren, M., Sévin, D., Wang, Y.-P., and Hwa, T. (2015). Inflating bacterial cells by  
273 increased protein synthesis. *Molecular Systems Biology*, 11(10):836.
- 274 Bennett, B. D., Kimball, E. H., Gao, M., Osterhout, R., Van Dien, S. J., and Rabinowitz, J. D. (2009). Absolute  
275 metabolite concentrations and implied enzyme active site occupancy in *Escherichia coli*. *Nature Chemical  
276 Biology*, 5(8):593–599.
- 277 Bremer, H. and Dennis, P. P. (2008). Modulation of Chemical Composition and Other Parameters of the Cell at  
278 Different Exponential Growth Rates. *EcoSal Plus*, 3(1).
- 279 Dai, X., Zhu, M., Warren, M., Balakrishnan, R., Okano, H., Williamson, J. R., Fredrick, K., and Hwa, T. (2018).  
280 Slowdown of Translational Elongation in *Escherichia coli* under Hyperosmotic Stress. - PubMed - NCBI. *mBio*,  
281 9(1):281.
- 282 Dai, X., Zhu, M., Warren, M., Balakrishnan, R., Patsalo, V., Okano, H., Williamson, J. R., Fredrick, K., Wang, Y.-P.,  
283 and Hwa, T. (2016). Reduction of translating ribosomes enables *Escherichia coli* to maintain elongation rates  
284 during slow growth. *Nature Microbiology*, 2(2):16231.
- 285 Fernández-Coll, L., Maciąg-Dorszynska, M., Tailor, K., Vadía, S., Levin, P. A., Szalewska-Palasz, A., Cashel, M.,  
286 and Dunny, G. M. (2020). The Absence of (p)ppGpp Renders Initiation of *Escherichia coli* Chromosomal DNA  
287 Synthesis Independent of Growth Rates. *mBio*, 11(2):45.
- 288 Godin, M., Delgado, F. F., Son, S., Grover, W. H., Bryan, A. K., Tzur, A., Jorgensen, P., Payer, K., Grossman, A. D.,  
289 Kirschner, M. W., and Manalis, S. R. (2010). Using buoyant mass to measure the growth of single cells. *Nature  
290 Methods*, 7(5):387–390.
- 291 Harris, L. K. and Theriot, J. A. (2018). Surface Area to Volume Ratio: A Natural Variable for Bacterial Morphogenesis.  
292 *Trends in microbiology*, 26(10):815–832.
- 293 JL, R., S, V., D, S., ÁD, O., A, S., and M, H. (2016). Bacterial Persistence Is an Active  $\sigma$ S Stress Response to Metabolic  
294 Flux Limitation. *Molecular Systems Biology*, 12(9):882.
- 295 Maaløe, O. (1979). *Regulation of the Protein-Synthesizing Machinery—Ribosomes, tRNA, Factors, and So On. Gene  
296 Expression*. Springer.
- 297 Milo, R., Jorgensen, P., Moran, U., Weber, G., and Springer, M. (2010). BioNumbers—the database of key numbers  
298 in molecular and cell biology. *Nucleic Acids Research*, 38(suppl\_1):D750–D753.
- 299 Schaechter, M., Maaløe, O., and Kjeldgaard, N. O. (1958). Dependency on Medium and Temperature of Cell Size  
300 and Chemical Composition during Balanced Growth of *Salmonella typhimurium*. *Microbiology*, 19(3):592–606.
- 301 Schmidt, A., Kochanowski, K., Vedelaar, S., Ahrné, E., Volkmer, B., Callipo, L., Knoops, K., Bauer, M., Aebersold,  
302 R., and Heinemann, M. (2016). The quantitative and condition-dependent *Escherichia coli* proteome. *Nature  
303 Biotechnology*, 34(1):104–110.
- 304 Scholz, S. A., Diao, R., Wolfe, M. B., Fivenson, E. M., Lin, X. N., and Freddolino, P. L. (2019). High-Resolution  
305 Mapping of the *Escherichia coli* Chromosome Reveals Positions of High and Low Transcription. *Cell Systems*,  
306 8(3):212–225.e9.
- 307 Scott, M., Gunderson, C. W., Mateescu, E. M., Zhang, Z., and Hwa, T. (2010). Interdependence of cell growth and  
308 gene expression: origins and consequences. *Science*, 330(6007):1099–1102.
- 309 Si, F., Le Treut, G., Sauls, J. T., Vadía, S., Levin, P. A., and Jun, S. (2019). Mechanistic Origin of Cell-Size Control  
310 and Homeostasis in Bacteria. *Current Biology*, 29(11):1760–1770.e7.
- 311 Si, F., Li, D., Cox, S. E., Sauls, J. T., Azizi, O., Sou, C., Schwartz, A. B., Erickstad, M. J., Jun, Y., Li, X., and Jun, S. (2017).  
312 Invariance of Initiation Mass and Predictability of Cell Size in *Escherichia coli*. *Current Biology*, 27(9):1278–1287.
- 313 Taheri-Araghi, S., Bradde, S., Sauls, J. T., Hill, N. S., Levin, P. A., Paulsson, J., Vergassola, M., and Jun, S. (2015).  
314 Cell-size control and homeostasis in bacteria. - PubMed - NCBI. *Current Biology*, 25(3):385–391.
- 315 Zhu, M. and Dai, X. (2019). Growth suppression by altered (p)ppGpp levels results from non-optimal resource  
316 allocation in *Escherichia coli*. *Nucleic Acids Research*, 47(9):4684–4693.